energy. Using the values of D_T and L, we can calculate an approximate value for the mean time between jumps; we find $\tau = 4 \times 10^{-9}$ s.

These results can be interpreted in the following way: the methanol molecules jump from one site to another, across the channel (they may rotate in a restricted geometry between the jumps), and they diffuse along the channels, after a large number of jumps, with a relatively low diffusion coefficient, 10^{-7} cm^2 s^{-1}. This value can be compared to the coefficient obtained for the diffusion of benzene in the channels of the mordenite, 2×10^{-6} cm^2 s^{-1},[11] and to the value obtained for the diffusion of ethylene in NaX, 3.1×10^{-6} cm^2 s^{-1}.[7]

VI. Discussion

On the time scale of IN6, i.e., 10^{-11}–10^{-12} s, we find that eight molecules out of ten are fixed per unit cell at 300 K. This value is in agreement with thermogravimetric results which indicate that seven methanol molecules are adsorbed per unit cell at 307 K on H-ZSM-5.[30] Furthermore, our result can be related to the adsorption of ammonia on the same zeolite;[4] it was found that nine molecules per unit cell are adsorbed at 293 K. In all these studies, it appears that, at room temperature, the number of adsorbed molecules (CH_3OH or NH_3) is greater than that attributable to the cations or hydroxyl groups. In this work, we have shown that our results are compatible with adsorption geometries B (Figure 3b) or C (Figure 3c). The self-association of the molecules can be discarded since in that case the EISF would drop more rapidly at low Q values.

We find that, in our temperature range, the methanol molecules do not react with the surface of H-ZSM-5 to produce methoxyl groups. This OCH_3 species would give exactly the same EISF as model 4, eq 15, but we have found that, as the temperature increases, a mobile species is progressively observed and this species corresponds to CH_3OH. This is in opposition to a methoxylation of the surface since this process appears to be enhanced when the temperature is increased.[31]

The highest temperature which we have studied is 425 K, that is, just below the beginning of dehydration of the alcohol giving dimethyl ether.[32] Again, if $(CH_3)_2O$ had been formed, the EISF would drop more rapidly. We find that, at 425 K, only three molecules per unit cell are fixed, which corresponds exactly to the number of hydroxyl groups in our sample (calculated from the chemical formula).

In the spheres of diameter 4.8 Å limited by the dimensions of the channels, the methanol molecules diffuse as fast as in the liquid since the value measured at 298 K in the liquid state is 2.4×10^{-5} cm^2 s^{-1}.[33] However, the long-range translational motion is much smaller in the zeolite (ca. 10^{-7} cm^2 s^{-1}) than in the liquid. Such behavior has already been reported in the case of water adsorbed in Nafion membranes.[34]

VII. Conclusion

From the point of view of neutron scattering, the molecular dynamics of methanol adsorbed on H-ZSM-5 is a complicated case. However, we have been able to characterize the rotational behavior of two methanol species: one fixed to the zeolite via hydrogen bonds and another diffusing within a volume restricted by the channel size. Such a model has also been recently proposed for the diffusion of hydrocarbons, in zeolite 5 A, measured by the frequency response method.[35] In this work, the translational motion has been interpreted in terms of jump diffusion (jump length $\simeq$ 5 Å) and a value of the diffusion coefficient at low Q, of the order of 10^{-7} cm^2 s^{-1}, has been found.

Acknowledgment. We thank Mr. G. Clugnet for his expert technical assistance during the preparation of the samples and Dr. G. J. Weiss of the Mobil Co. for supplying the ZSM-5.

Registry No. Methanol, 67-56-1.

(30) Ison, A.; Gorte, R. J. *J. Catal.* **1984**, *89*, 150.
(31) Salvador, P.; Kladnig, W. *J. Chem. Soc., Faraday Trans. 1* **1977**, *73*, 1153.
(32) Nováková, J.; Kubelková, L.; Habersberger, K.; Dolejšek, Z. *J. Chem. Soc., Faraday Trans. 1* **1984**, *80*, 1457.
(33) Hurle, R. L.; Easteal, A. J.; Woolf, L. A. *J. Chem. Soc., Faraday Trans. 1* **1985**, *81*, 769.
(34) Volino, F.; Pineri, M.; Dianoux, A. J.; De Geyer, A. *J. Polym. Sci., Polym. Phys. Ed.* **1982**, *20*, 481.
(35) Yasuda, Y.; Yamamoto, A. *J. Catal.* **1985**, *93*, 176.

Zero-Field NMR of Solid Bis(μ-hydrido)decacarbonyltriosmium

D. B. Zax,[†] A. Bielecki, M. A. Kulzick,[‡] E. L. Muetterties,[§] and A. Pines*

Department of Chemistry, University of California, and Materials and Molecular Research Division, Lawrence Berkeley Laboratory, Berkeley, California 94720 *(Received: July 25, 1985)*

In this work, zero-field proton NMR is applied to a polycrystalline sample of bis(μ-hydrido)decacarbonyltriosmium ((μ-H)$_2$Os$_3$(CO)$_{10}$). Bis(μ-hydrido)decacarbonyltriosmium is of interest as a model for small-molecule–surface interactions. The solid-state structure makes it a good test compound for zero-field NMR methods. The internuclear dipole–dipole interactions are used as a probe of structure. Where high-field NMR methods cannot generally be applied to the study of large numbers of coupled spins, even in disordered (e.g. polycrystalline) materials zero-field NMR may result in analyzable spectra. The solid-state powder spectrum of (μ-H)$_2$Os$_3$(CO)$_{10}$ is analyzed to give proton–proton distances which are compared with the results obtained from single-crystal diffraction methods.

Introduction

The determination of molecular structure is of paramount importance in a variety of chemical disciplines. While a vast array of techniques are commonly available for structure determination, only a few can be applied to solids and yet fewer may be used to obtain detailed geometrical information in the solid state. For studies requiring such information, one must usually resort to methods employing X-ray or neutron diffraction. These techniques, although powerful, are time-consuming and expensive and also require single crystals in order to uniformly diffract the X-ray or neutron beam. Growing single crystals can be a major problem. Moreover, X-rays cannot reliably locate hydrogen nuclei. Thus the development of a technique which is applicable to polycrystalline samples is very important. In this paper, such a technique

[†] Present address: Isotope Division, Weizmann Institute of Science, Rehovot, Israel.
[‡] Present address: Amoco Research Center, P. O. Box 400, Naperville, IL 60566.
[§] Deceased.

0022-3654/86/2090-1065$01.50/0

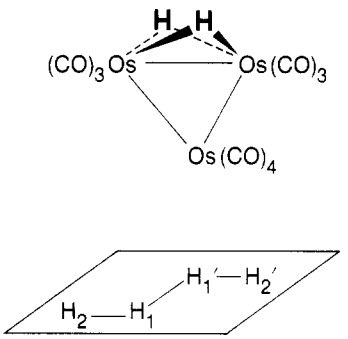

Figure 1. Structure of $(\mu\text{-H})_2Os_3(CO)_{10}$ in the solid state. Upper: Approximate molecular geometry. Lower: Simplified representation, showing only the arrangement of hydrogen atoms within the unit cell. The relatively close grouping of the four hydrogens and the inversion symmetry of the unit cell make this view appropriate.

is discussed; we report a contribution to the question of the hydrogen atom locations within the crystalline framework, based on a study of a polycrystalline sample of bis(μ-hydrido)decacarbonyltriosmium, $(\mu\text{-H})_2Os_3(CO)_{10}$ (Figure 1), by zero-field NMR.[1,2] Where normal high field NMR tends to give broad unresolved spectra in disordered solids, zero field NMR can produce relatively sharp spectra with resolved features characteristic of the molecular geometry.

$(\mu\text{-H})_2Os_3(CO)_{10}$ was selected for this study for several reasons. The compound is of some importance in organometallic chemistry. It is a starting material for the synthesis of a variety of osmium carbonyls. Due to its high affinity for unsaturated organics, it has been used as a model for small-molecule–surface interactions.[3] The chemistry at the hydrogen atom sites is itself interesting; they are believed to occupy positions equidistant between two osmium atoms, and it is likely that they participate in three-center bonds. Additionally, its structure and chemistry have been probed by a number of techniques, including both single-crystal X-ray and neutron diffraction[4-6] and photoelectron spectroscopy.[7] Details of the chemistry and bonding in heavy-metal hydrides have been derived from a number of techniques, including a number of NMR studies, both in the solid state and in solution.[8-13] Thus the accuracy of the zero-field NMR technique can be assessed.

Here we concentrate on the application of zero-field NMR to the specific question of ^1H–^1H distances in the solid state, and we comment on their relation to the more general question of the arrangement of the protons within the crystalline framework. These distances can be derived from the NMR spectrum because the observed spectral features arise predominantly from the dipolar couplings between the spin $^1/_2$ nuclei of the hydrogen atoms. These couplings are determined by internuclear distances, angles, and motional factors, and therefore are characteristic of the skeleton of the high magnetogyric ratio, spin $^1/_2$ nuclei. Where small groupings of such nuclei are well-isolated from all others, solid-state NMR techniques should be capable of providing detailed structural information even where only powdered or disordered samples are available. This is precisely the sort of spin system expected in metal–carbonyl clusters.

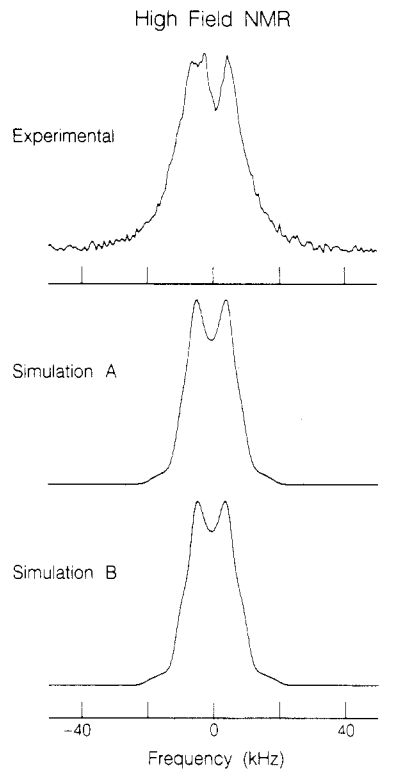

Figure 2. High-field proton NMR spectra of polycrystalline $(\mu\text{-H})_2Os_3(CO)_{10}$. Upper: Experimental spectrum obtained by the dipolar echo sequence (90_x–τ–90_y–τ–acquire). Center and lower: Computer simulations of the high-field powder patterns, assuming only the effects of homonuclear dipolar couplings; specifically, the effects of chemical shift anisotropy are neglected. The assumed internuclear distances are summarized in Table I.

TABLE I: Internuclear Distances Assumed in Simulations, in Å[a]

proton pair	simulation A	simulation B
1–1′	2.94	2.81
1–2	2.38	2.38
1–2′	5.28	5.17

[a] Given the assumed inversion symmetry of the unit cell, all other proton–proton distances are uniquely determined.

High-Field NMR of $(\mu\text{-H})_2Os_3(CO)_{10}$

A number of previous NMR powder and solution studies of metal–carbonyl clusters have been performed. Information about bonding and ligand dynamics has been derived by using ^{13}C chemical shifts[8] and J couplings,[9] ^{17}O relaxation times,[10] and ^1H solid-state chemical shift tensors as probes.[11] In ordered phases, the spectrum is dominated by the near-neighbor dipolar interaction, and therefore one would expect it to be a source of direct structural information. This fact was previously exploited in a structural study of a ruthenium hydride cluster by nematic phase proton magnetic resonance.[12] The high-field NMR spectrum of $(\mu\text{-H})_2Os_3(CO)_{10}$, obtained at a ^1H frequency of 185 MHz, is shown in Figure 2. Unfortunately, the observed powder pattern only poorly approximates the shape predicted for two interacting nuclei and is complicated by the presence of sizable chemical shifts. The high-field spectrum is too poorly resolved to allow for any direct interpretation in terms of interproton distances. An earlier attempt to interpret the spectrum based on the assumption that it arose from only two coupled spins gave inconsistent results.[13]

The simulated high-field powder patterns in Figure 2, and the hypothetical structures on which they are based, are discussed in a later section where a comparison is made to the associated

(1) (a) D. P. Weitekamp, A. Bielecki, D. Zax, K. Zilm, and A. Pines, *Phys. Rev. Lett.*, **50**, 1807 (1983). (b) D. B. Zax, A. Bielecki, K. W. Zilm, and A. Pines, *Chem. Phys. Lett.*, **106**, 550 (1984). (c) D. B. Zax, A. Bielecki, K. W. Zilm, A. Pines, and D. P. Weitekamp, *J. Chem. Phys.*, **83**, 4877 (1985).
(2) (a) A. Bielecki, J. B. Murdoch, D. P. Weitekamp, D. B. Zax, K. W. Zilm, H. Zimmermann, and A. Pines, *J. Chem. Phys.*, **80**, 2232 (1984). (b) D. B. Zax, A. Bielecki, A. Pines, and S. W. Sinton, *Nature (London)*, **312**, 351 (1984).
(3) P.-K. Wang, C. P. Slichter, and J. H. Sinfelt, *Phys. Rev. Lett.*, **53**, 82 (1984).
(4) M. R. Churchill, F. J. Hollander, and J. P. Hutchinson, *Inorg. Chem.*, **16**, 2697 (1977).
(5) A. G. Orpen, A. V. Rivera, E. G. Bryan, D. Pippard, G. M. Sheldrick, and K. D. Rouse, *J. Chem. Soc., Chem. Commun.*, 723 (1978).
(6) R. W. Broach and J. M. Williams, *Inorg. Chem.*, **18**, 314 (1979).
(7) D. E. Sherwood and M. B. Hall, *Inorg. Chem.*, **21**, 3458 (1982).
(8) S. Aime, D. Osella, L. Milone, and E. Rosenberg, *J. Organometal. Chem.*, **213**, 207 (1981).
(9) S. Aime and D. Osella, *J. Chem. Soc., Chem. Commun.*, 300 (1981).
(10) S. Aime, R. Gobetto, D. Osella, L. Milone, G. E. Hawkes, and E. W. Randall, *J. Chem. Soc., Chem. Commun.*, 794 (1983).
(11) A. T. Nicol and R. W. Vaughan, *J. Am. Chem. Soc.*, **101**, 583 (1979).
(12) A. D. Buckingham, J. P. Yesinowski, A. J. Canty, and A. J. Rest, *J. Am. Chem. Soc.*, **95**, 2732 (1973).
(13) A. T. Nicol and R. W. Vaughan, *Adv. Chem. Ser., No. 167*, 248 (1978).

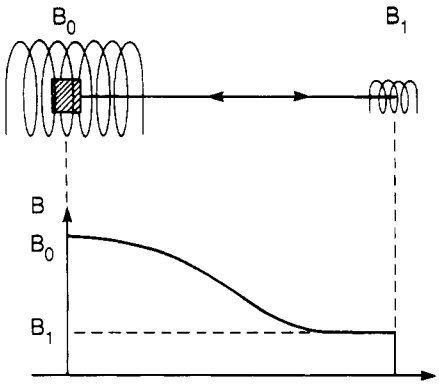

Figure 3. Schematic representation of the zero-field NMR technique. The larger field B_0 (42 kG) is used to prepare a nuclear magnetization at the beginning of the field cycle. Then the sample is shuttled to the intermediate field B_1 (100 G), where the field can be rapidly switched to zero. After an interval of zero-field evolution, traditionally called t_1, the field B_1 is switched back on and the sample brought back to B_0 where the magnetization may be measured. The field cycle is repeated with regularly incremented values of t_1 to measure the zero-field evolution of the magnetization.

zero-field spectra. The structures assumed in the simulations are summarized in Table I.

Principles of Zero-Field NMR

In high-field NMR, the single largest contribution to the energy spectrum is the interaction of the magnetic moments of the nuclei with the externally applied field. The individual nuclear spins are quantized along the field; all other terms which reflect the local fields (e.g. chemical shifts and J couplings in high-resolution NMR) are observed only as perturbations on the much larger Zeeman energy splittings. In the solid state, the observed local fields are dominated by anisotropic contributions, which in liquid or gaseous systems are averaged to zero by rapid, diffusive motions. In the absence of these motions, the energy levels which characterize the nuclear spin states for some set of spins (say an isolated group in a crystallite) acquire an explicit dependence on the relative orientation between that set of spins and the applied magnetic field. Perturbation theory is therefore appropriate to describe the effect of the dipolar field arising from a single nuclear spin on its neighbors. For homonuclear spin systems, the truncated first-order dipole–dipole Hamiltonian is (in frequency units, Hz)

$$H_d^0 = -\sum_{i<j} \frac{\gamma^2 h}{8\pi^2 r_{ij}^3}(3\cos^2\theta_{ij} - 1)(3I_{zi}I_{zj} - I_i \cdot I_j) \qquad (1)$$

where θ_{ij} is the angle between the laboratory z axis (chosen along the applied field) and the internuclear vector, $\mathbf{r}_{ij}$. Each crystallite in a powder (or otherwise each unique orientation in any disordered system) is characterized by a unique set of energy levels and transition frequencies. The observed spectrum corresponds to a continuous distribution of such frequencies, with each orientation contributing with a statistical weight given by its probability. For all but the simplest systems, this spectrum is a broad and rather featureless band.

In contrast, in the absence of an applied field, the Hamiltonian which arises from the local fields alone is identical for all subsystems which differ from one another only by translations, reflections, and rotations in space. The untruncated dipolar Hamiltonian is

$$H_d = \sum_{i<j} \frac{\gamma^2 h}{4\pi^2 r_{ij}^3}\left(I_i \cdot I_j - \frac{3}{r_{ij}^2}(I_i \cdot \mathbf{r}_{ij})(I_j \cdot \mathbf{r}_{ij})\right) \qquad (2)$$

What is important to note is that there is no orientation dependence of the energy levels in this Hamiltonian. Each crystallite has the same energy level structure and therefore can give rise to only one set of transition frequencies.

Zero-field NMR spectroscopy requires the use of the modifications and attachments described in more detail elsewhere.[14] The method is summarized schematically in Figure 3. The zero-field spectrum is acquired by a point-by-point technique. The sample is polarized by allowing it to equilibrate in high field for a time comparable to T_1, the spin–lattice relaxation time, and is shuttled on a stream of high-pressure air to a field of ~100 G. This field is rapidly (~1 μs) shut off and the bulk magnetization is allowed to evolve in zero applied field for a period of time called t_1. The 100-G field is then reapplied, and the sample transported to high field where the amplitude of the evolved magnetization is sampled by standard high-field NMR techniques. Each data point represents the evolution of the spin system in zero field for a fixed time t_1, and each value of the signal function $S(t_1)$ is measured by repeating the entire field cycle.

At the time $t_1 = 0$, the point in the field cycle when the externally applied field is turned off, the Hamiltonian (and thus the energy splittings) are identical for all sets of equivalent spins. What differs from one set to the next is rather the orientation of the nuclear magnetization, prepared in high field parallel to the axis of the applied field, as expressed in some consistently chosen local axis system. Because magnetization is not an equilibrium form of nuclear spin order in zero field, the magnitude of the magnetization becomes time-dependent. The evolution of this magnetization in the presence of the local fields is analogous to the normal FID observed in high-field NMR experiments. Precession can only occur at those frequencies characteristic of the untruncated local fields, and this results in the greatly increased resolution of the zero-field technique.

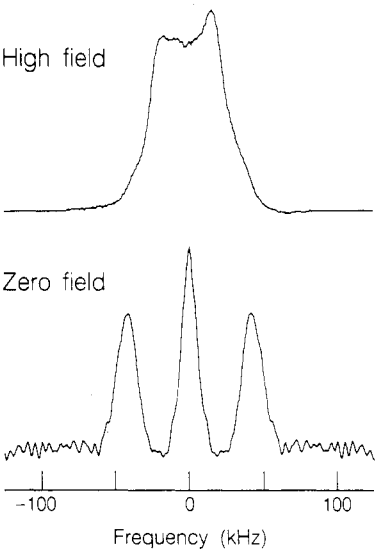

Figure 4. Proton NMR spectra of $CaCl_2 \cdot H_2O$. Upper: High-field spectrum obtained by the $(90_x\text{–}\tau\text{–}90_y\text{–}\tau\text{–acquire})$ dipolar echo sequence. Lower: Zero-field spectrum obtained by the experimental method described in the text. The zero-field spectrum indicates that the protons are arranged in isolated pairs, with an internuclear distance of approximately 1.6 Å.

Resolution of Zero-Field Spectroscopy: $CaCl_2 \cdot 2H_2O$

As an example of the resolution advantage of zero-field NMR, consider a two-spin system. In Figure 4 we present both high- and zero-field spectra of $CaCl_2 \cdot 2H_2O$. The high-field spectrum (top) is similar to that presented in Figure 2; other than a small dip in the center of the spectrum, there is little resolved structure. This is often true of high-field proton dipolar spectra. The ideal two-spin Pake pattern, with sharp singularities and its characteristic line shape, is only rarely observed experimentally due to complications from nonvanishing couplings to all other spins in the lattice, and other interactions present in high field such as the chemical shift. Moreover, complicated spin systems may mimic the same general behavior, exhibiting local minima in the center of the absorption band. For $CaCl_2 \cdot 2H_2O$, the zero-field

(14) A. Bielecki, D. B. Zax, K. W. Zilm, and A. Pines, *Rev. Sci. Instrum.*, in press.

spectrum (bottom) clearly shows the three-line spectrum predicted to arise from the dipolar interaction between two homonuclear spins in zero field[1] and indicates that the couplings between pairs of protons in separate water molecules are sufficiently weak that the main spectral features are described by the simple two-spin model. These extended couplings contribute primarily to the breadth of the observed zero field lines. In clusters of strongly coupled sets of dipolar-coupled nuclei, the spectral features are dominated by the strongest couplings (i.e. those within each cluster) even when some of the couplings between spins in two different clusters are as large as the smallest of those within a single cluster. It is reasonable to treat each cluster as a system and to treat couplings between clusters as a broadening term.

Experimental Section

$(\mu\text{-H})_2Os_3(CO)_{10}$ was prepared according to the method of Knox et al.[15] The sample was purified by recrystallization from *n*-hexane and vacuum-dried to remove excess solvent. Approximately 100 mg was recovered and packed in a Kel-F NMR sample tube. The solid-state ^1H NMR spectra were acquired with a homebuilt spectrometer and superconducting magnet system operating at a frequency of 185 MHz. High-field spectra were accumulated by using a dipolar echo sequence to remove the effects of finite receiver recovery time. The free induction decay (FID) was sampled at 6-μs intervals which afforded a spectral bandwidth of 166 kHz. The dipolar echo sequence may lead to some distortions in the observed spectrum when more than two spins are coupled together.[16] Therefore, the time interval between the pair of pulses was kept to a minimum.

The zero-field spectra were acquired with the technique described above. The polarization and detection phases took place in the same superconducting magnet system used in acquiring the high-field spectra except for the necessary adaptations for zero-field NMR spectroscopy.[14] The sample was polarized by allowing it to approach equilibrium in a high field for 1 min. Transit to and from the zero-field region requires ~150 ms. The length of the time period t_1 is controlled digitally by the same clock which oversees all functions of the high-field spectrometer. In this experiment, t_1 ranged from 0 to 1275 μs in regular increments of 5 μs (giving an effective bandwidth of 200 kHz). After the 100-G field was reapplied and the sample transported to high field, the amplitude of the evolved magnetization was sampled by standard high-field NMR methods. For simplicity, the signal $S(t_1)$ can be considered to be equal to the initial amplitude of the evolved magnetization after a single rf pulse; in practice, application of a simple multiple-pulse sequence (pulsed spin locking[17]) in high field extends the decay period of the high-field signal from ~50 μs in the absence of these additional pulses to several milliseconds. During the decay period the magnetization may be sampled many times; by averaging the data thus obtained, the signal-to-noise ratio is greatly increased as compared to simpler detection schemes which only measure the initial height of the decay. For each field cycle, the averaged signal is taken as representative of the corresponding value of t_1. A total of 256 t_1 points were accumulated and constituted the zero-field free induction decay. Eleven such free induction decays were summed and Fourier transformed to yield the spectrum of Figure 5. One-half the full spectral width is shown.

Results and Discussion

The zero-field spectrum of polycrystalline $(\mu\text{-H})_2Os_3(CO)_{10}$ shown in Figure 5 should be contrasted to the normal high-field spectrum of Figure 2. In the zero-field spectrum, we resolve a large number of lines. Unlike the zero-field spectrum of $CaCl_2\cdot H_2O$ shown in Figure 4, the observed features cannot be described by assuming only a simple model of two interacting spins. Intermolecular couplings are so large that they, too, must be explicitly considered. Crystal structures[4-6] reveal two molecules per unit cell related by an inversion center. We use the observed crystalline symmetry as a basis for locating the nearest neighbors within the unit cell. This, in fact, enables us to place the hydrogen atom network within the crystal lattice, which would not be possible if the only observed interactions arose from pairs within a given molecular unit.

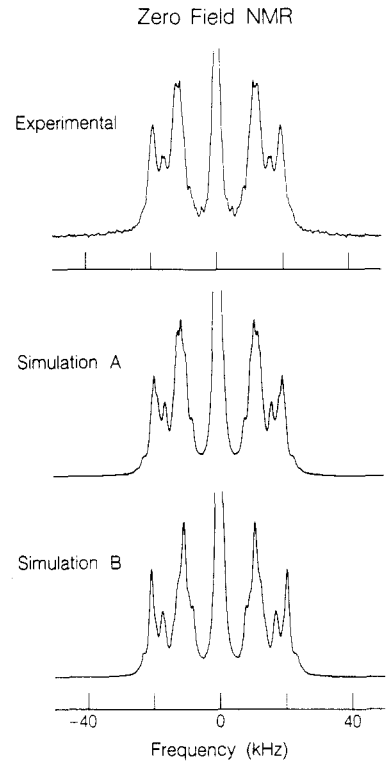

Figure 5. Zero-field proton NMR spectra of polycrystalline $(\mu\text{-H})_2Os_3(CO)_{10}$. Upper: Experimental spectrum obtained by the method described in the text. Center: Computer simulation which is our best fit to the experimental spectrum. Lower: Simulation based on the internuclear distances reported in ref 6, a low-temperature neutron diffraction study. The proton–proton distances assumed for the simulations are given in Table I.

Simulations of zero-field spectra are based on an algorithm described in detail elsewhere.[1c] Basically, given a set of atomic coordinates, the Hamiltonian of eq 2 can be expanded and diagonalized. The differences between eigenvalues of the Hamiltonian correspond to the transition frequencies while intensities are related to the representation of the magnetization vector in the eigenbasis of the zero-field Hamiltonian. This algorithm results in a zero-field spectrum which consists of a number of discrete lines at precise frequencies. These "stick spectra" are broadened to match the observed line widths, which are due to couplings not explicitly included in the model and lifetime broadening. In practice, the experimentally observed line shapes are best reproduced by assuming a Lorentzian line shape, which suggests that the lifetime effects dominate. In the simulations in Figure 5, the assumed Lorentzian line width is 2.8 kHz.

As a basis for comparison, the atomic coordinates derived from a low-temperature neutron diffraction study[6] are used to produce simulation B of Figures 2 and 5. These coordinates provide a passable fit to the observed high-field spectrum but are clearly an inadequate representation of the zero-field spectrum. Also in Figures 2 and 5 is a simulation for a different relative orientation of the four hydrogen nuclei which much more closely fits the observed data. The simulated high-field powder patterns (Figure 2) based on the same two structures scarcely differ.

Dipole–dipole couplings between one cluster of four ^1H nuclei in one unit cell and clusters in other unit cells are insufficient to explain the observed deviations between the simulated and experimental spectra. While there is one rather close intercell ^1H–^1H

(15) S. A. R. Knox, J. W. Koepke, M. A. Andrews, and H. D. Kaesz, *J. Am. Chem. Soc.*, **97**, 3942 (1975).
(16) P. Mansfield, *Phys. Rev.*, **137**, A961 (1965).
(17) (a) E. D. Ostroff and J. S. Waugh, *Phys. Rev. Lett.*, **16**, 1097 (1966). (b) W.-K. Rhim, D. P. Burum, and D. D. Elleman, *Phys. Rev. Lett.*, **37**, 1764 (1976). (c) D. Suwelack and J. S. Waugh, *Phys. Rev. B*, **22**, 5110 (1980). (d) M. M. Maricq, *Phys. Rev. B*, **25**, 6622 (1982).

distance (5.09 Å based on the low-temperature neutron diffraction study[6]) this dipole–dipole coupling is much smaller than the assumed line width. Furthermore, the evolution of one spin in the field of its neighbors is dominated by the very strongest couplings, and therefore the interaction of an isolated nucleus a distance $\bar{r}$ from a cluster is much greater than of one spin in a cluster with spins in a second cluster.

When molecular motion is significant, some care must be taken in interpreting the derived distances, as the distances derived in an NMR experiment are not in general the mean distances.[18] Depending upon the nature of the vibrational mode, the NMR value may be either longer or shorter than the diffraction values. Because the molecular framework is quite rigid (evidence for which is provided by the relatively long spin–lattice relaxation time, which is ~1 min) the spectral analysis is unlikely to be complicated by any sort of motional averaging, and the simulations are based on the assumption of no molecular motion.

The intramolecular distance we derive is approximately that of the low-temperature neutron diffraction study; the distance between the pairs in the unit cell is quite a bit larger than predicted from the same study,[6] and also larger than the value derived from the X-ray data at room temperature.[4] (Late in the preparation of this work, we received a list of atomic coordinates by private communication with the authors of ref 5; our results agree with theirs somewhat more closely than with those of ref 4 and 6.) Knowledge of the interpair distance serves to partially locate the four-proton network within the crystal lattice, as the center of the line connecting pairs of crystallographically equivalent nuclei must correspond to the center of the unit cell (however, the orientation with respect to the crystal axes cannot be obtained in our powder analysis). The primary difference between our coordinates and those of the neutron study is that the intermolecular interaction seems somewhat weaker. This corresponds to the observed shrinkage of the unit cell at low temperatures.[6]

(18) (a) S. Meiboom and L. Snyder, *Acc. Chem. Res.*, **4**, 81 (1971). (b) S. Sykora, J. Vogt, H. Bosiger, and P. Diehl, *J. Magn. Reson.*, **36**, 53 (1979). (c) J. Lounila and P. Diehl, *Mol. Phys.*, **52**, 827 (1984).

Conclusions

In this work we have shown the application of zero-field NMR to determine reasonable internuclear distances for the protons in a magnetically dilute system. Polycrystalline $(\mu\text{-H})_2Os_3(CO)_{10}$ was chosen as a test compound because it is a relatively simple spin system with a well-characterized structure, and because there is interest in its chemical behavior. Zero-field NMR studies at room temperature reveal an apparent expansion in the crystal lattice as compared to the results of neutron diffraction data done on a single crystal at a lower temperature. This result is consistent with temperature-dependent studies of the density of this compound. All of the crystal lattice expansion seems concentrated in the weakening of the intermolecular contacts. For small numbers of coupled spins, zero-field NMR has also been shown to provide information about the approximate numbers of interacting spins, where normal high-field NMR techniques are much less definitive.

Acknowledgment. D. B. Zax was supported by a National Science Foundation Graduate Fellowship, and M. A. Kulzick was supported by the National Science Foundation through Grant CHE-83-07159. This work was supported by the Director, Office of Energy Research, Office of Basic Energy Sciences, Materials Sciences Division of the U.S. Department of Energy, and the Director's Program Development Funds of the Lawrence Berkeley Laboratory, under Contract DE-AC03-76SF00098.

Registry No. $(\mu\text{-H})_2Os_3(CO)_{10}$, 41766-80-7.

The Structure and Spectral Properties of a Squarylium Dye, 2,4-Bis[(1-*n*-butyl-2(1*H*)-quinolylidene)methyl]-1,3-cyclobutadienediylium-1,3-diolate

J. Bernstein,†

Department of Chemistry, Ben-Gurion University of the Negev, Beersheva 84120, Israel

M. Tristani-Kendra,‡ and C. J. Eckhardt*†

Department of Chemistry, University of Nebraska—Lincoln, Lincoln, Nebraska 68588-0304
(Received: August 12, 1985)

Structural and spectral characterizations of the title compound, 2,4-bis[(1-*n*-butyl-2(1*H*)-quinolylidene)methyl]-1,3-cyclobutadienediylium-1,3-diolate (BQMS), a prime candidate for a solar energy material, have been carried out. Crystals are monoclinic, $P2_1/n$ with $a = 9.586$ (2) Å, $b = 9.730$ (2) Å, $c = 13.894$ (3) Å, $\beta = 99.77$ (9)°, and $Z = 2$. The structure has been solved by direct methods and refined by using 1078 reflections for which $F > 2\sigma(F)$ with anisotropic temperature factors on the non-hydrogen atoms to $R = 0.098$ and $R_w = 0.074$. Quasi-metallic reflection is observed along both principal directions for the (101) and (001) faces. The transition moment is found to be polarized along the long axis of the molecule.

Introduction

The squarylium class of organic dyes has received a great deal of attention recently due to their potential application in solar energy conversion,[1-3] electrophotographic processes,[4] photovoltaic cells,[5] and optical storage systems.[6] An understanding of the relationship between the structure and optical and electronic properties of these materials is crucial if they are to be designed

†Supported, in part, by the U.S.-Israel Binational Science Foundation and the Department of Energy under Grant No. DE-FG-02-79ER10535.

‡Work completed in partial fulfillment of requirements for the Ph.D. at the University of Nebraska—Lincoln. Present address: 3M Co., St. Paul, MN 55144-1000.

(1) Morel, D. L. *Mol. Cryst. Liq. Cryst.* **1979**, *50*, 127.
(2) Forster, M.; Hester, R. E. *J. Chem. Soc., Faraday Trans. 1* **1982**, *78*, 1847.
(3) Morel, D. L.; Ghosh, A. K.; Feng, T.; Stogryn, E. L.; Shaw, P. E.; Fishman, C. *Appl. Phys. Lett.* **1978**, *32*, 495.
(4) Metz, P. J.; Champ, R. B.; Chang, L. S.; Chiou, C.; Keller, G. S.; Liclian, L. C.; Neiman, R. R.; Shattuck, M. D.; Weiche, W. J. *Photogr. Sci. Eng.* **1977**, *21*, 73.

0022-3654/86/2090-1069$01.50/0